

ANALYSIS OF MEASURED IN-FLIGHT TAIL LOADS

P.A. van Gelder
 National Aerospace Laboratory NLR
 Anthony Fokkerweg 2
 NL-1059 CM Amsterdam, The Netherlands

Abstract

Fatigue load spectra that are used for the design of aircraft tail structures are based on usually simplifying assumptions with respect to aircraft usage, payload, manoeuvres, external disturbances (turbulence), and aircraft response behaviour. Past service-load measurement programs have been restricted to measuring the vertical acceleration of aircraft at the centre of gravity, which gives ample information about main wing loads but lacks a proper correlation with tail loads. In general the relation between aircraft tail loads and aircraft motion parameters (lateral or vertical acceleration, pitch or yaw rate) is insufficient. Therefore the best way to obtain this information is by direct measurement of these tail loads by means of calibrated strain gauges.

A measurement program was carried out, to obtain data for validating the procedures currently being used for the determination of tail load spectra and to improve the knowledge of the statistics of gust and manoeuvres relevant to tail loads. In this programme, tail loads have been obtained from a commercially operated Fokker 100 aircraft in service with KLM Royal Dutch airlines. Special attention was paid to the measurement set-up, since neither interference with other aircraft systems, nor adverse effects on the availability of the aircraft were permissible. This was taken care of using a combined system for the recording of data. A number of relevant parameters already recorded by the existing Aircraft Condition Monitoring System were combined with load parameters recorded by a dedicated stand-alone data recorder. This data recorder was operated without any interference with other aircraft systems. The tail structure was instrumented with a number of strain gauges in order to measure the bending moments of one stabilizer half and their symmetrical and anti-symmetrical components. Lateral accelerations at the rear fuselage were also measured.

This paper describes the measurement of the various parameters, the creation of a database containing more than 2000 flights and analysis of the results.

Comparison of measured load spectra with design/test spectra enabled a validity check of the design procedures and confirmed the conservatism of the assumptions that have been made.

Introduction

The National Aerospace Laboratory NLR has a long standing tradition in the application of smart data recorders for in-flight fatigue-load monitoring ^(1,2) especially for military aircraft ^(3,4) and helicopters ^(5,6) and application of Digital Flight Data Recorders of commercially operated civil aircraft for instance for acquiring gust statistics ^(7,8,9). This paper describes the analysis of measured data in which both experiences have been applied to create a database of more than 2000 flights with unique information that can be used for the validation of procedures that are applied to determine fatigue load spectra in the design phase of aircraft.

Problem statement. In order to obtain fatigue-load spectra for the design of aircraft tail structures a number of usually simplifying assumptions are made in order to account for the effects of aircraft usage and payload, external disturbances (turbulence), control inputs and aircraft response behaviour.

The derived spectra cannot easily be verified, at least not with measured data, since service-load measurement programs that have been conducted in the past were mainly concentrated on measuring and registration of vertical accelerations of the aircraft at the centre of gravity. These accelerations are a good measure of main-wing loads, but the correlation with tail loads is usually poor. In general the relation between aircraft tail loads and aircraft motion parameters is insufficient for the derivation of tail loads and tail load spectra.

Solution. Therefore the best and most direct way to obtain aircraft tail loads is by measurement using calibrated strain gauges. To this purpose a measurement program was started in the Netherlands in order to validate the procedures that are currently used for the determination of tail load spectra and to improve the statistical knowledge of gusts and manoeuvres, with respect to tail loads.

In this measurement program tail loads have been obtained from a commercially operated Fokker 100 aircraft (Fig. 1) in service with a Dutch airline company (KLM). Special attention was paid to the measurement set-up, since neither interference with other systems nor adverse effects on the availability of the aircraft were permissible.

This dilemma was solved by using a combined system for

the recording of data. A relevant number of aircraft parameters, already recorded by the existing Aircraft Condition Monitoring System (ACMS), were combined with loads parameters recorded by a stand-alone dedicated data recorder. This data recorder was operated without any interference to other aircraft systems. The tailplane was instrumented with a number of strain gauges in order to measure the bending moments of one stabilizer half, and its symmetrical and anti-symmetrical component. The strain gauges were calibrated by the manufacturer (Fokker Aircraft BV) before mounting the stabilizer to the vertical fin structure. Also lateral accelerations of the rear fuselage were measured.



Fig. 1 Fokker 100 tail structure

Measurement of tail loads

The continuity of the Fokker 100 tail-loads measurement program had its up's and downs due to changes in operations and operators^(10,11) but halfway 1995 a database with more than 2000 flights had been created.

Instrumentation and calibration

In order to quantify tail loads, bending moments at the root of the horizontal tail were considered to be of prime interest. In order to measure these bending moments nine strain gauge bridges (3 shear- and 6 tension bridges) were

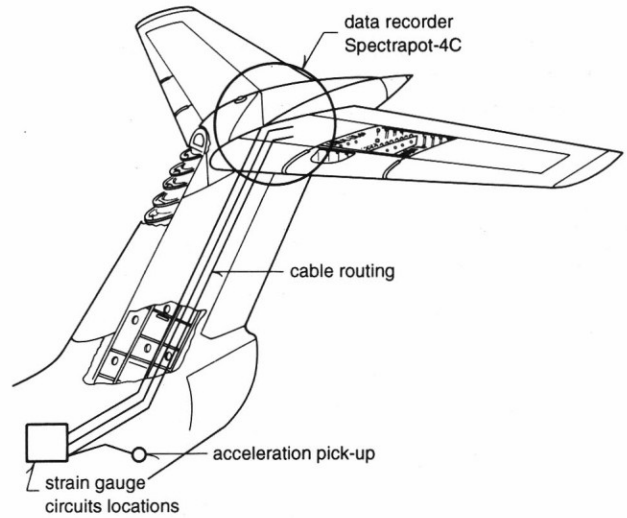
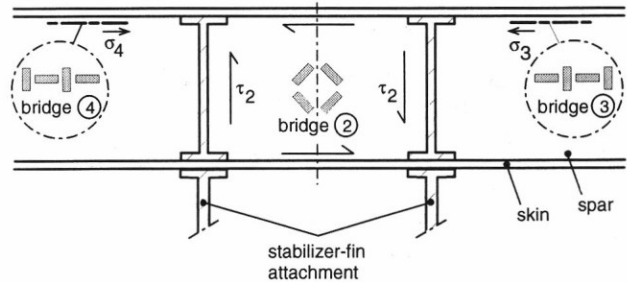


Fig. 2 Lay-out of the instrumentation in the tail of the Fokker 100



	symmetric loading condition	anti-symmetric loading condition
shear bridge (2)	$\tau_2 = 0$	$\tau_2 \neq 0$
tension bridges (3), (4)	$\sigma_3 = \sigma_4$	$\sigma_3 = -\sigma_4$
(3) + (4)	$\sigma_3 + \sigma_4 \neq 0$	$\sigma_3 + \sigma_4 = 0$
(3) - (4)	$\sigma_3 - \sigma_4 = 0$	$\sigma_3 - \sigma_4 \neq 0$

Fig. 3 Strain-gauge type and -location in relation to measured output

installed in the root section of the horizontal stabilizer of a Fokker 100 aircraft (Fig's. 2 and 3). More than the minimum required number of strain gauges were installed in order to have some spare gauges in case of malfunctioning or breakdown during testing or operation. Installation of the bridges, accelerometer and cables, as well as the calibration of the instrumentation in order to establish the strain-bending moment relationship, was carried out by Fokker Aircraft BV. The calibration was performed on the stabilizer before it was attached to the aircraft. The gauges were chosen in such a way that the following loads could be measured:

- the bending moment of one stabilizer half (bmom),
- the symmetrical part of this bending moment (symm),
- the anti-symmetrical part of this bending moment (asym).

A lateral accelerometer was installed in the tail of the aircraft in order to establish a possible correlation between lateral accelerations and anti-symmetric tail loads and for the derivation of lateral gust loads. The sign-convention for the bending moments and the accelerations is depicted in figure 4.

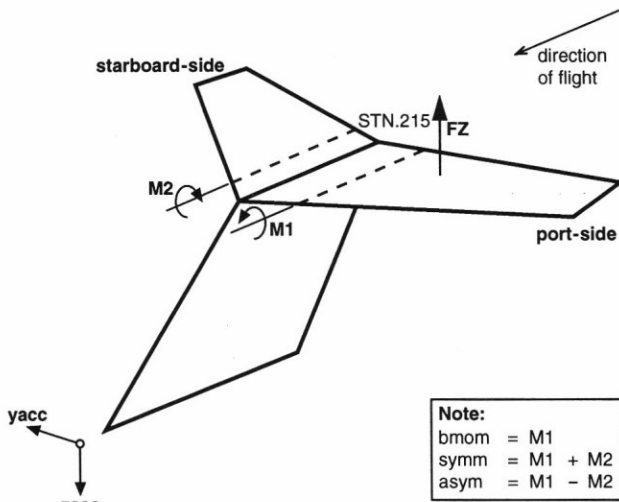


Fig. 4 Sign convention for tail loads

Recording of loads data (SPECTRAPOT-4C)

The tail load measurements were carried out during normal operation of the aircraft. The measurements were carried out with a compact micro-processor based recording device (Spectrapot-4C, Fig. 5), mounted in the tail cone of a Fokker 100 aircraft. With this particular data-recorder four independent input signals can be digitized, processed

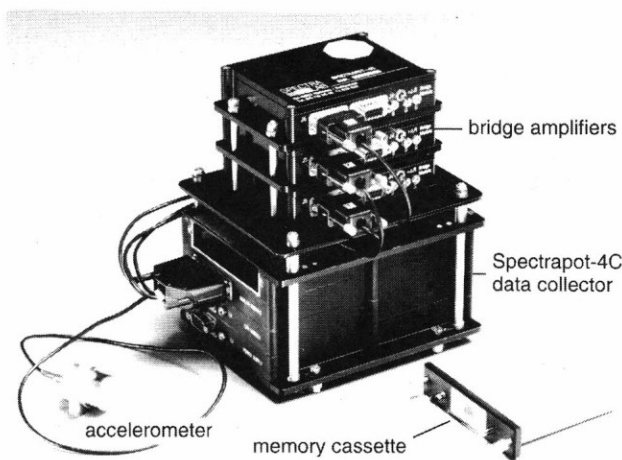


Fig. 5 Spectrapot-4C data recorder

and recorded for further analysis.¹⁾ One of the major advantages of this device is the stand-alone capability which does not require interconnection with other aircraft systems (other than power supply and on/off switching).

After filtering and sampling, the signals were searched for 'peaks' and 'valleys' with a given range-filter size. Successive values are stored into the solid state memory, including time marks. The solid state memory was changed regularly, approximately at a weekly basis.

Recording of aircraft- and flight parameters (ACMS)

KLM operated Fokker 100 aircraft are equipped with a so-called Aircraft Condition Monitoring System (ACMS) which stores a large number of aircraft, engine and flight parameters on the Digital Airborne Recorder (DAR).

All recordings consist of data frames with a duration of four seconds, equally divided into four mini-frames of one second each.

From all recorded parameters 28 have been selected by NLR for further processing (Tab. 1). The data pertaining to these

Table 1 Parameters obtained from ACMS database

Parameter	Parameter
1 Aircraft Id	15 Pitch angle
2 Date	16 Elevator position
3 Time	17 Aileron position
4 Flight number	18 Mach number
5 Flight count	19 Roll angle
6 Int. Subframe nr.	20 Rudder position
7 Gross weight	21 Hor. Stabilizer pos.
8 Fuel weight	22 TE flap position
9 Flight mode	23 EPR engine #1
10 True Airspeed	24 EPR engine #2
11 True Heading	25 T/R engine #1
12 Angle of Attack	26 T/R engine #2
13 Pressure altitude	27 Stable frame flag
14 Centre of gravity	28 Vert. CG acceleration

Table 2 ACMS definition of flight modes

FM	Flight mode	Remarks
1 PC	Pre-flight	
2 ES	Engine start	
3 TA	Taxi before take-off	FM ⁻¹ =ES, V < 60 knots
	after touch-down	FM ⁻¹ =RO, V < 60 knots
4 TO	Take-off	ground
5 CL	(initial) Climb	FM ⁻¹ =TO, alt < 2500 ft
		Vv > 300 ft/min
6 ER	En Route	airborne, alt > 2500 ft
7 AL	Approach & landing	airborne, alt > 2500 ft
		Vv < -300 ft/min
8 RO	Rollout	ground, V > 60 knots
9 GA	Go-around	
Note:	FM ⁻¹ previous flight mode	V Computed airspeed
	Vv Vert. speed inertial	alt Radio altitude

¹⁾ The more recent version of this recorder allows for 16 channels and increased memory capacity.

selected parameters were extracted from the ACMS flight-tapes by the computing centre of the aircraft operator. A brief description of ACMS flight mode definition is given in table 2.

Database creation

A database has been created containing the recorded information for each flight. To that purpose the Spectrapot and ACMS data had to be combined. A diagram of the dataflow is presented in figure 6.

In order to facilitate data-inspection, data-plotting, data-correction, data-merging and data-reduction, a program-suite has been established which comprises these functions. Also the ACMS recorded data have been subjected to further data reduction before they were entered into the database. For instance during 'cruise' when most parameters remain constant for a long time there is no need to keep the data at small time intervals. Another example is the vertical cg-acceleration, which is stored by ACMS eight times per second is processed by a 'peak/valley' algorithm and entered into the database similarly to the loads parameters ('range-filter' = 0.1 g). The data has been checked and corrected for out-of-range values, data-spikes and 'glitches'. Special attention has been given to the synchronization between sub-frame numbers and the time-parameters.

Data synchronisation

Since the data originates from two un-coupled data-sources, with different internal clocks, the resulting information is most likely to be out-of-sync (not synchronised). In order

to get a proper synchronisation between the two data sources, ACMS is chosen to be the reference and the Spectrapot data is corrected with a time-shift. This time-shift is based on the assumption that the peaks in (symmetric) tail plane bending moment and elevator signal during take-off should be simultaneous. Due to the resolution of the ACMS elevator/time-parameter (1 second), and the accuracy of the Spectrapot time-parameter (+/- 1 second), the synchronisation will not be better than $\pm 1-2$ seconds.

During the process of database-creation 'summary-file' with relevant flight information is created and 'error-reports' are produced to identify parameters that have been corrected in the process and could be un-reliable. From this 'summary-file' flight statistics can be derived very easily for instance:

- distribution of flight/block time,
- distribution of take-off/landing weight,
- flap usage statistics,
- elevator/rudder/aileron usage statistics,
- speed/altitude distribution,
- etc.

The database has been created with the intention to verify assumptions being made for design-fatigue load spectra in the design phase of aircraft. Therefore a database with relevant flight and loads information has been created which may be different from 'usual' flight measurements in a sense that no time traces (at equally spaced time intervals) are stored, but mainly extreme values (peak/valleys) with a time-mark.

From this information it is very well possible to distinguish the essential flight-phases (load-wise) and the Ground-Air-Ground cycle. This is illustrated in the following example of a typical time-history.

Typical time-history

From the recorded signals some typical points relating to specific flight conditions can be observed (Fig. 7):

- After engine start and taxiing to the runway, power is applied, which can be seen from the increase in the engine pressure ratio (epr, point 1→2). When power is applied the control column is pushed forward (positive elevator deflection) to keep the aircraft's nose down. When speed has increased the aircraft is rotated by an elevator angle of approximately -10 deg. (elev, point 2). Rotation of the aircraft during take-off is associated with a (negative) peak in the symmetrical bending moment (symm, point 2). After take-off engine power is initially decreased but increases gradually when the aircraft climbs to cruising altitude (alt, point 3). During cruise the bending moment reduces to small values, which implies that the required (negative) tail load for aircraft equilibrium is rather small.
- Engine power is cut back (epr & alt, point 4) to start the descent. Speed is reduced before the landing flaps can be extended. During the low-speed and flap-in condition the bending moment gets very small (symm, point 5) because the balancing force in this condition

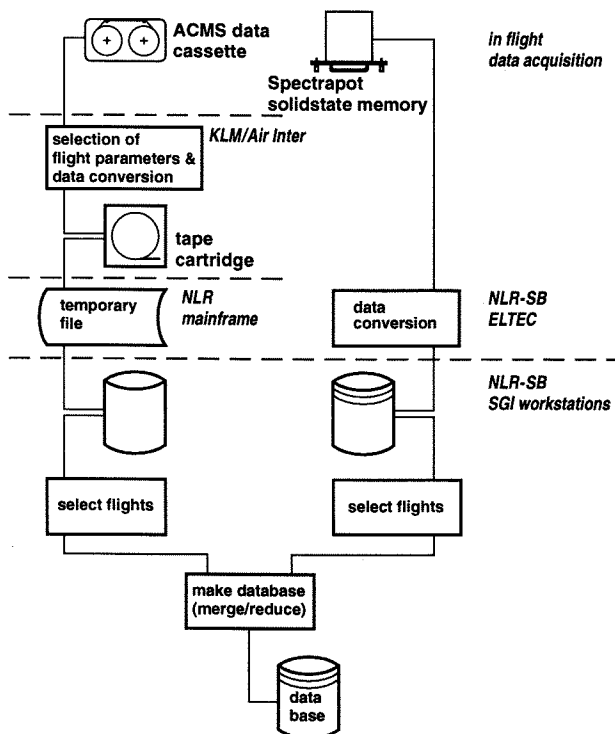


Fig. 6 Flow diagram of the creation of the database

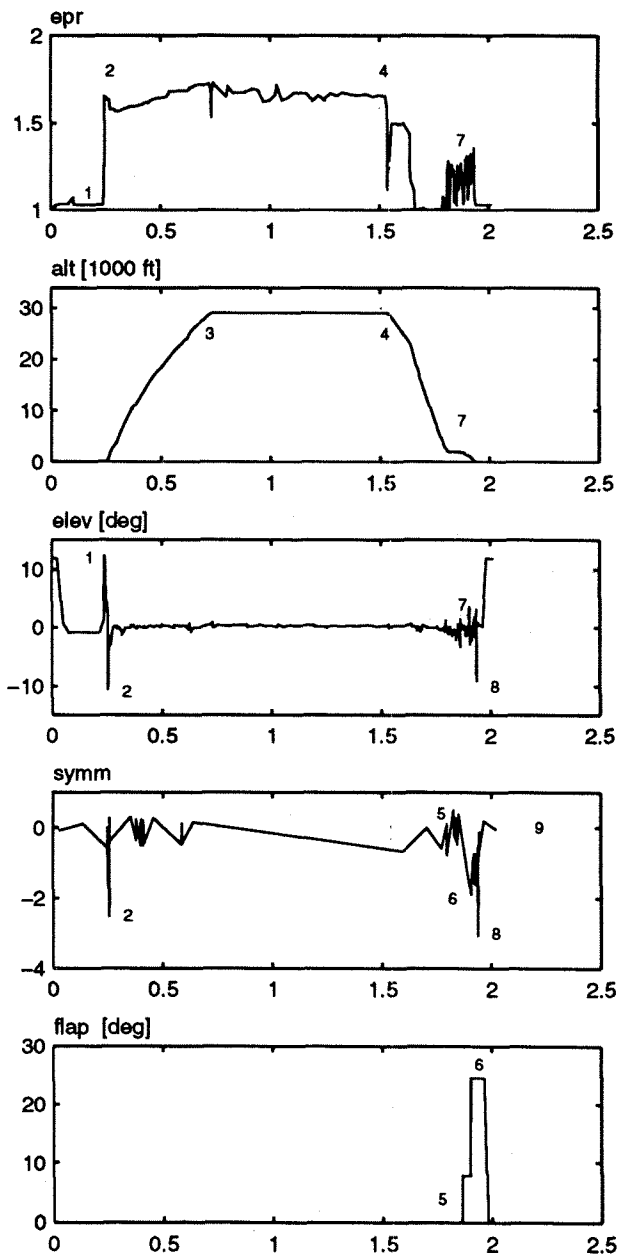


Fig. 7 Typical time-histories (db_1528)

is very small. When the flaps are extended to 25 degrees (flap, point 6) the bending moment decreases (to a larger negative value) due to the larger balancing load (symm, point 6). A lot of activity is noticed in both the engine signal (epr, point 7) and in the elevator signal (elev, point 7) in order to maintain course on the glide path. A distinct peak in bending moment (symm, point 8) is visible during the flare manoeuvre, which coincides with maximum elevator deflection (elev, point 8).

The bending moment gradually decreases to approximately zero during landing and roll-out (symm, point 8→9).

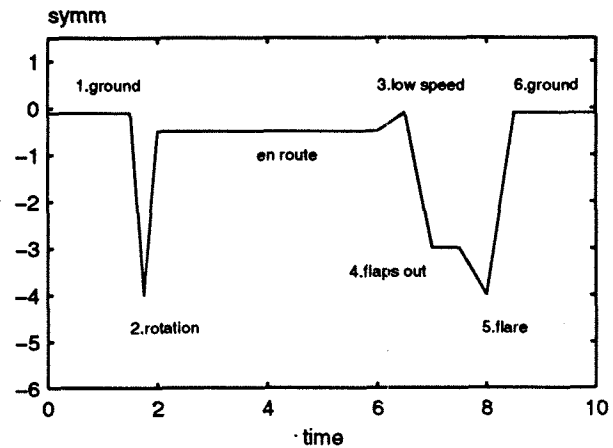


Fig. 8 Simplified Ground-Air-Ground cycle for the symmetric tail plane bending moment

Generally speaking the Ground-Air-Ground (GAG) cycle for the symmetrical tail bending moment consists of two load cycles. Starting from zero on the ground (Fig. 8, point 1) the load increases to a peak during the rotation manoeuvre at take-off (Fig. 8, point 2), then the bending moment is more or less constant during the flight, followed by a valley due to the balancing load at low speed and flaps in (Fig. 8, point 3). During the final approach with flaps in landing position (Fig. 8, point 4) the bending moment increases and on top of that a peak occurs during the flare manoeuvre (Fig. 8, point 5) followed by a valley during zero load on the ground (Fig. 8, point 6).

Analysis of flight loads

The analysis that will be presented in this paper will concentrate on the following topics:

- load-factor spectrum
- tail-load spectra
- usage statistics in relation to the 'equivalent flight'

The load spectra that will be presented are derived from recorded (reduced) time histories that are transferred into peak-valley sequences first before applying the so-called 'Range-Pair Range' counting method.⁽²⁾

Load factor-spectrum

From the spectrum of vertical accelerations at the centre of gravity of the aircraft, expressed in the form of a load factor (measured acceleration, normalized by the acceleration of gravity), a general impression can be obtained whether or not the batch of flights is more or less 'normal' and representative for the usage of a Fokker 100. In figure 9 the spectrum for 'airborne' modes (FM = 5,6,7,9) is presented in combination with the Fokker 100 design spectrum. The difference between measured spectrum and design spectrum is the result of the Fokker philosophy, where the design

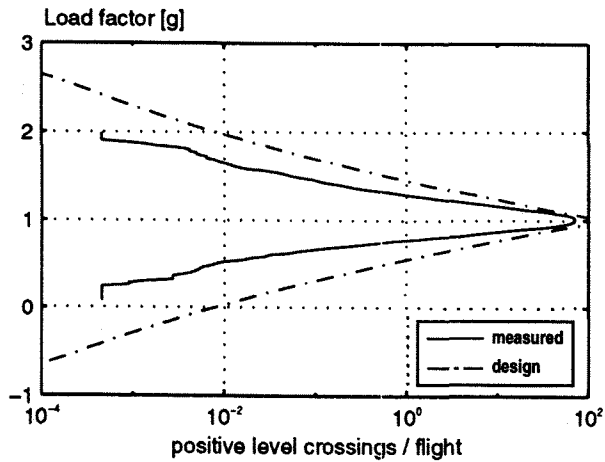


Fig. 9 Load factor spectrum (airborne)

('equivalent flight') has been defined in such a way that it represents 'severe' usage rather than average usage. This is clearly demonstrated by the load factor spectrum for the Fokker F28 in comparison to measured spectra (fatigue meter readings) from the most severe (max) and least severe (min) operator (Fig. 10).

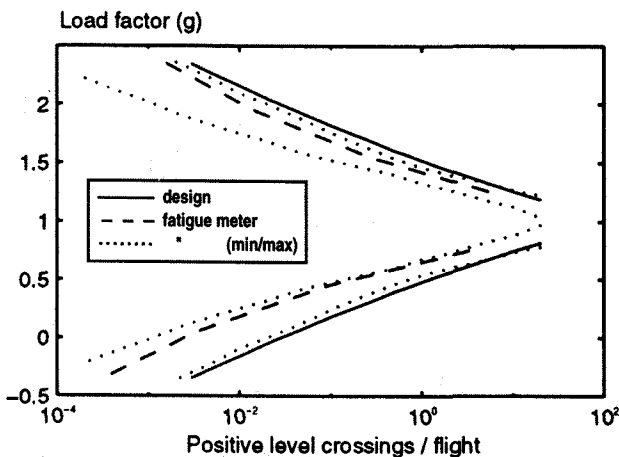


Fig. 10 F28 load factor spectrum

Since the measured load factor spectrum is well within the design spectrum and has a regular shape it is concluded that the batch of flights does not contain extraordinary flight conditions or flight conditions with heavy (wing) loads, however it should be noted that although the spectrum is based on 2000 flights it is still related to only two operators and a particular type of operation (short-haul flights in Western Europe).

Also the load factor spectrum for ground modes is presented (Fig. 11). It is noticed that the measured loads are much smaller than assumed in the design spectrum.

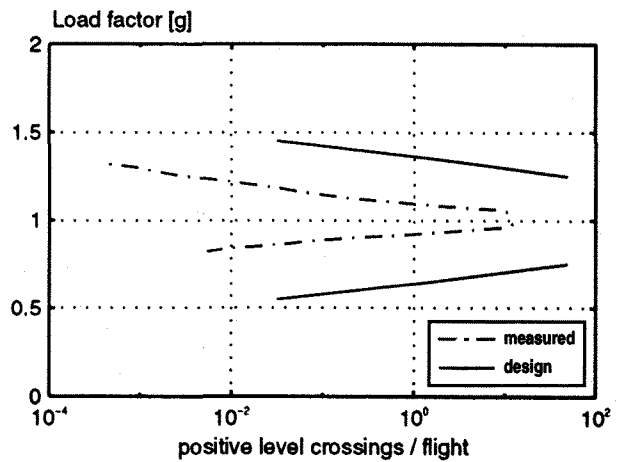


Fig. 11 Load factor spectrum (ground/taxiing)

Tail load spectra

Tail load spectra are presented for the root-bending moment of one stabilizer half (bmom), its symmetrical (symm) and its anti-symmetrical part (asym), in comparison to the load spectra that have been applied in the full-scale fatigue test of the Fokker 100 tail structure that has been carried out by NLR. In this way the overall results can be compared, which gives a global indication about the validity of the assumptions being used in the process of developing design fatigue-load spectra. A better comparison could be made by modifying the 'design' load spectra according to the statistical results found from the database, e.g. the number and severity of manoeuvres, gust encounters, actual weight, cg acceleration etc. This is not possible however, since only the overall load spectra are available at NLR.

bmom-spectrum

In figure 12a and 12b the load spectrum for the total stabilizer root bending moment (bmom) is presented as cumulative positive-level-crossings and cumulative number of ranges respectively. These spectra are related to all data (airborne + ground modes). From the shape of the positive-level-cross spectrum (Fig. 12a) it is seen that the measured spectrum has two different 'peaks' which are related to different static aircraft equilibrium conditions (flaps in/out) with a rather regular shape. In the design spectrum more of these 'peaks' are present due to more differing equilibrium conditions being accounted for. The 'peak' around zero bending moment is caused by anti-symmetric load cases (roll-out after landing with thrust reverse application) with a very small mean-value (≈ 0) of bending moment.

Also the equilibrium loads in the design spectrum are larger than found from the measurements. The difference in equilibrium conditions is caused by a conservative approach in the assumptions for the design spectrum, especially with respect to cg-position and flap-usage, see also next section

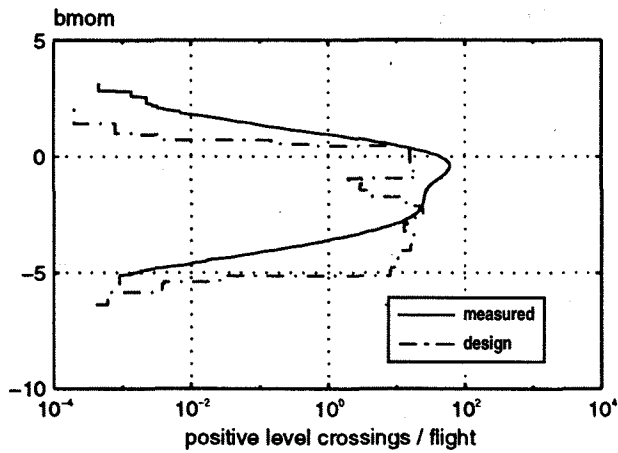


Fig. 12a *bmom-spectrum (level crossings)*

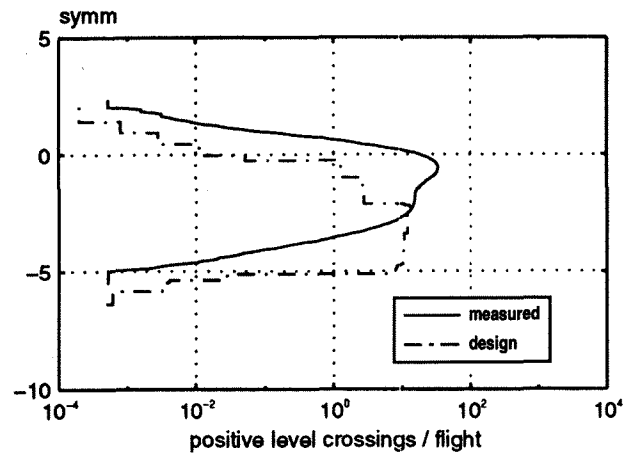


Fig. 13a *symm-spectrum (level crossings)*

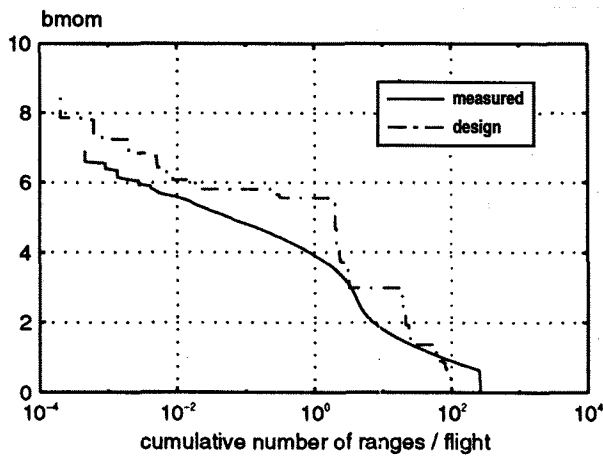


Fig. 12b *bmom-spectrum (ranges)*

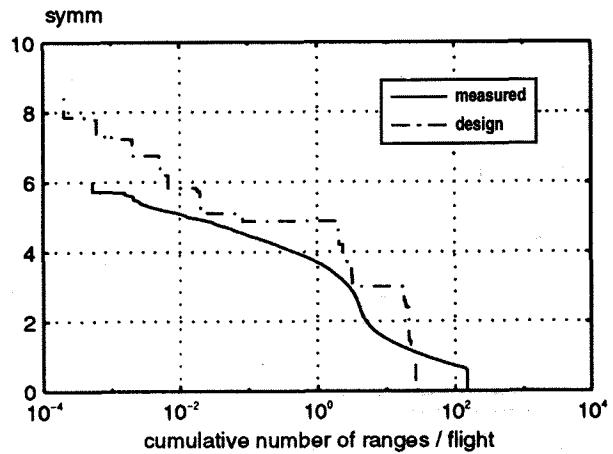


Fig. 13b *symm-spectrum (ranges)*

'equivalent flight'.

From the range-spectrum (Fig. 12b) it is seen that the main Ground-Air-Ground cycle with two peaks (two cycles) per flight (see also Fig. 8) for symmetric loads is also noticeable in the total bending moment and that the design load is approximately 1.5 times larger than the measured load (bmom). The design spectrum does not contain small loads that occur very frequently (more than 100 times/flight). The load level that occurs ± 20 times per flight corresponds to (symmetric) elevator manoeuvres.

symm-spectrum

The load spectrum for the symmetrical part of the stabilizer root bending moment (symm) is also presented as cumulative positive-level-crossings and cumulative number of ranges (Fig. 13a and 13b respectively). The same observation as for the previous load spectrum (bmom) can be made, the most frequent measured equilibrium condition (approx. -1.0) is much smaller than the design spectrum (approx. -3.0). Also in the range spectrum a large margin

(factor ± 1.5) at the load-range that occurs twice per flight is present.

The load level that occurs ± 20 times per flight corresponds to (symmetric) elevator manoeuvres, and is also found in the bmom-spectrum.

asym-spectrum

The load spectrum for the anti-symmetrical part of the stabilizer root bending moment consists of lateral gust loads, anti-symmetric manoeuvre loads, such as decrabbing before landing, loads due to thrust-reverser application etc. It is important to mention that this anti-symmetrical part of the bending moment (top-roll moment) causes the main loading of stabilizer to vertical tail attachment fitting.

The asym level-cross spectrum (Fig. 14a) itself is symmetric. The range spectrum (Fig. 14b) shows that the loads occurring once per flight are very well captured by the design spectrum, although with a smaller margin (± 1.15) than the symmetric (symm) and total (bmom) loads.

The load level that occurs ± 30 times per flight corresponds

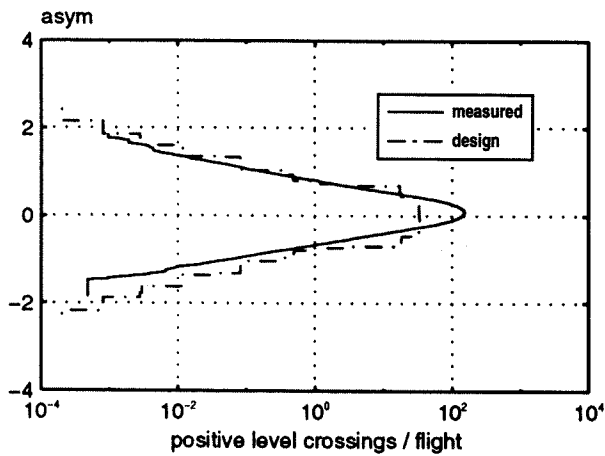


Fig. 14a asym-spectrum (level crossings)

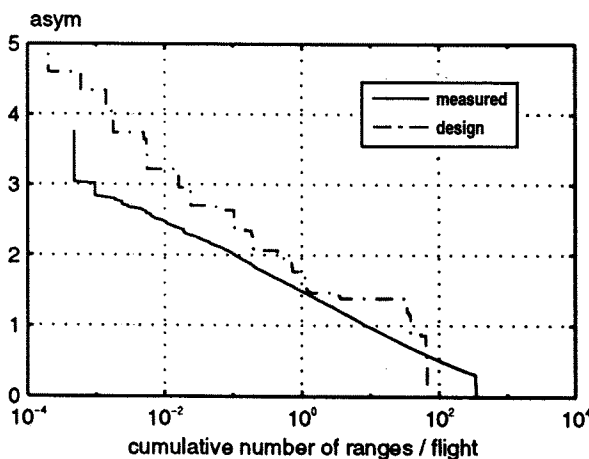


Fig. 14b asym-spectrum (ranges)

to thrust reverser loads during roll-out.

'Equivalent flight'

The 'equivalent flight' is a virtual flight profile that is used as the basis for the majority of fatigue load spectra. This flight profile is chosen in such a way, that the fatigue load exposure is equivalent to an aircraft which predominantly performs 'heavy' missions with respect to fatigue.

Some aspects of conservatism are included into the determination of the equivalent flight, mainly in the approach and landing phase which has great impact on the fatigue load spectra:

- low altitudes, with more turbulence (more encounters and more severe);
- high airspeeds, giving rise to higher loads;
- long approach segments (including 10 minutes holding per 10 flights) with long manoeuvring times, more turbulence and high flap-fatigue loading;
- full flap landing, resulting in high tailplane loads and high flap loads;
- forward cg-location in flight, according to passenger seating preferences and resulting in high tailplane and aft-fuselage loads;

Table 3 Some database statistics in relation to the 'equivalent flight'

		Eq.fl.	\bar{x}	σ_n
Flight duration	(hrs)	0.55	1.10	0.43
Block time	(hrs)	-	1.36	0.43
Take-off weight	(10^3 kg)	37.6	38.7	2.6
Fuel weight	(10^3 kg)	3.9	4.2	1.9
max. flap take-off	(deg)	15	4.1	4.0
min. cg-location (6)	(% \bar{c})	15.0	22.7	3.2
max. altitude	(10^3 ft)	23	28.4	7.0
Landing weight	(10^3 kg)	36.2	36.3	2.2
min. cg-location (7)	(% \bar{c})	14.9	22.6	3.2
max. Mach number	(-)	0.70	0.71	0.06
max. flap	(deg)	42	38.2	7.2

Note:
 Flight duration: time between lift-off and touch down
 Block time: time between 'Engine Start' (FM=2) and end of 'Taxi after landing' (FM=3)
 Take-off weight: weight at time of lift-off (begin of FM=4)
 Landing weight: weight at time of touch-down (end of FM=7)
 Fuel weight: fuel weight at time of lift-off (begin of FM=4)
 minimum cg (6): minimum cg-location during "en route" (FM=6)
 minimum cg (7): minimum cg-location during "approach/landing" (FM=7)
 max. altitude: maximum altitude during "en route" (FM=6)
 max. Mach: maximum Mach number during "en route" (FM=6)
 max. flap: maximum flap angle during "approach/landing" (FM=7)

- short flight duration and minimum cost schedules for operation, resulting in low fuel consumption, low Take-off fuel weight and consequently high wing bending moments.

Some of these assumptions are checked whether they are conservative or not, by comparing parameters from the 'equivalent flight' with average values (\bar{x}), standard deviations (σ_n) and the minimum and maximum occurring values found from the database (table 3).

The average flight duration (1.10 hrs) is longer than the 'equivalent flight' (0.55 hrs). Although it has been assumed for the equivalent flight that a short flight duration would result in a lower wing weight due to less fuel, the difference in fuel weight is only 300 kg. This means that the assumption is right but only marginally conservative.

The average cg-location during 'En Route' (FM=6) and 'Approach & Landing' (FM=7) is more aft (8 % \bar{c}) than assumed for the 'equivalent flight'. This means that the balancing load ($nz=1$) during those flight phases will be smaller, resulting in smaller (static) bending moments of the stabilizer. This is also observed in the load spectra (level crossings) for the stabilizer bending moment (Fig. 12a & 13a).

The assumption that this would imply a (very) conservative approach is not confirmed by the measured load spectra in terms of load-ranges. The load range spectrum (important for fatigue) is in good agreement with the design spectrum regardless the more aft cg-position (Fig.12b & 13b).

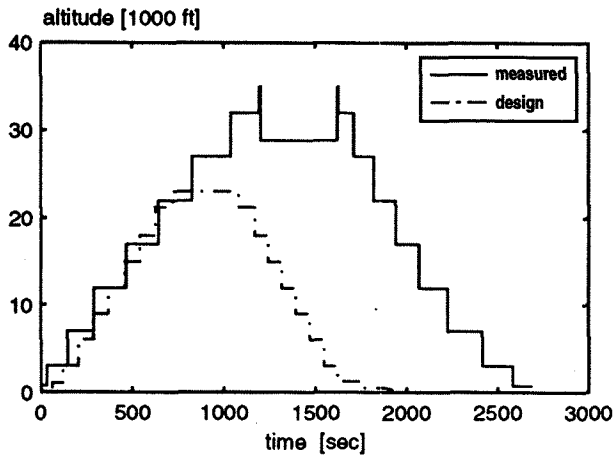


Fig. 15a Time spent per altitude band

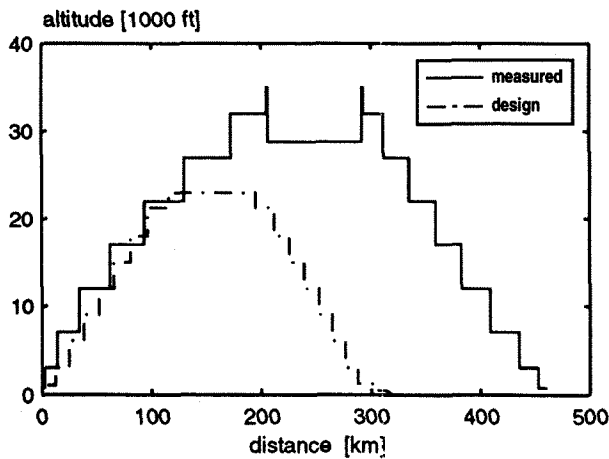


Fig. 15b Distance travelled per altitude band

Time-spent or distance-travelled in different altitude bands is presented in figure 15a & 15b respectively. A distinction has been made between climbing, cruising and descending in order to get results that can be compared with the 'equivalent flight'. The average maximum altitude is much higher than for the 'equivalent flight'.

The average landing weight (36,300 kg) is almost the same as the assumed landing weight for the 'equivalent flight' (36,200 kg). It is not known how this affects the spectrum for landing loads.

The flap-position during take-off (8 deg.) differs from the 15 deg. that has been assumed for the 'equivalent flight'. The average value of all flights amounts to 4.1 degrees, because the flaps are used only in 52% of all cases (table 3). This also means that the assumption for the equivalent flight is conservative for wing and flap loads. Static tail-plane loads however will be smaller due to a reduced balancing force during take-off.

The 'equivalent flight' assumes long approach segments (10 minutes holding per 10 flights). This is a conservative assumption, when average flap-extend times are compared to the flight segments holding/approach from the 'equivalent flight'. The 'equivalent flight' assumes a total flap extend time for holding and approach of 270 sec, while the average

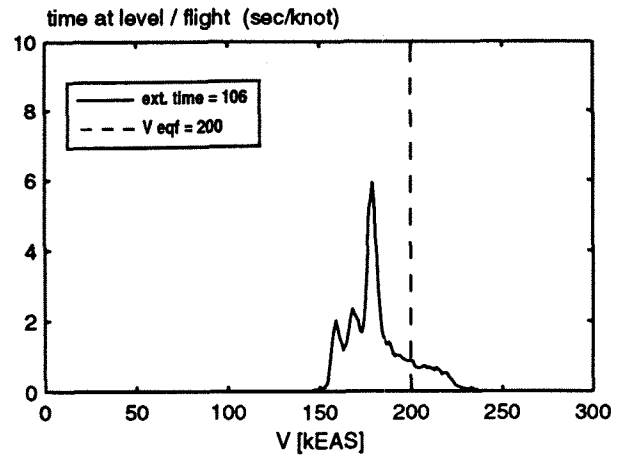


Fig. 16a Speed distribution (Flap=8 deg)

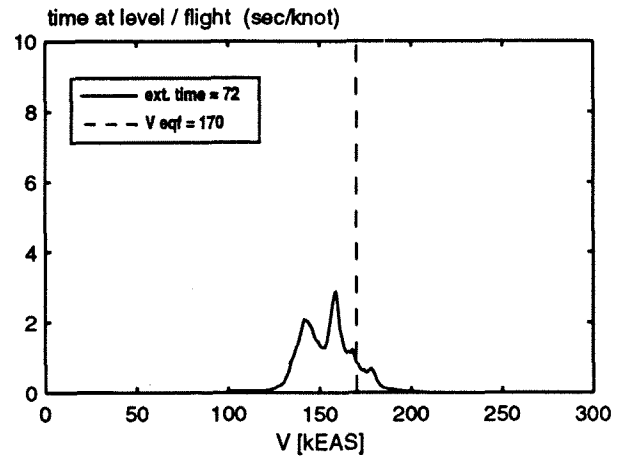


Fig. 16b Speed distribution (Flap=25 deg)

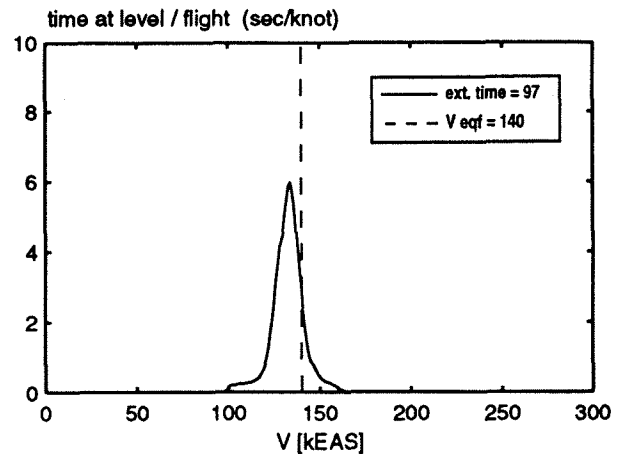


Fig. 16c Speed distribution (Flap=42 deg)

measured flap extend time (8 & 25 degrees) is less than 178 sec (Fig. 16) because also landings with 25 deg. flap have been carried out. The average speeds when flying with 25 or 42 degrees flap is much lower than assumed for the 'equivalent flight', which means a conservative approach with respect to gust loads.

The average of the maximum flap angle during approach and landing (38.2 deg.) is not equal to the maximum possible flap angle of 42 degrees. In 22% of the landing cases a maximum flap-position of 25 degrees has been selected (table 4b).

In figure 16a,b,c the 'time-at-level' of flap positions 8, 25 and 42 deg, during approach/landing are presented.

For 25 degrees flap (Fig. 16b) it is observed, that two peaks are present. One relates to the approach phase, the other to the landing phase. Both peaks compare very well with the assumed speeds from the equivalent flight.

For full flap selection (42 deg) the actual airspeed is less than 140 kEAS in 83% of the time that the flaps are extended in that position.

Table 4a Flap selection per flight during take-off

Flap angle (deg)	Total	%
0	986	48
8	1069	52

Table 4b Flap selection per flight during landing

Flap angle (deg)	Total	%
25	449	22
42	1606	78

This means that the high airspeed assumption for full flap landings is conservative with respect to the design speed (180 kEAS) and realistic with respect to the equivalent flight assumptions (140 kEAS) as far as the full flap landings are concerned. Landing with 25 degrees flap and the same landing speeds means that the assumed flap loads will be conservative.

Furthermore balancing loads will be smaller resulting in smaller (static) tail-plane forces and bending moments.

So the following conclusions are made with respect to wing and tailplane loads:

- Flap and wing loads will be (slightly) conservative,
- Static tail-plane loads (bending moments) will be smaller due to conservative assumptions with respect to cg-position and flap usage,

- Approach and landing speeds are in good agreement with the 'equivalent flight' assumptions so there will be no conservatism in the speed effect in relation to gust loads during approach and landing.
- The duration of the time spent in the holding/approach segment is less than assumed, so the 'equivalent flight' is conservative with respect to possible gust encounters for this flight segment.

Conclusions

- A system has been described for the recording of tail loads during operational flights, which makes use of the aircraft ACMS in combination with a stand-alone 'smart' data recorder. This recorder can be operated without interference to other aircraft systems. In this way a database of more than 2000 flights has been created.
- The number of flights in the database is assumed to be sufficient to provide useful information with respect to usage and loads statistics.
- The measured loads and other flight data made it possible to check the validity and confirmed the conservatism of procedures that are used for the determination of fatigue-load spectra.

Acknowledgement

The investigations described in this paper have been carried out under contract with the Netherlands Agency for Aerospace Programs (NIVR) in cooperation with Fokker Aircraft BV and KLM Royal Dutch Airlines.

References

- 1 J.B. de Jonge, "The monitoring of fatigue loads", Paper presented at ICAS-Congress, Rome 1970, also NLR MP 70010, September 1970.
- 2 J.B. de Jonge, "The analysis of Load-Time histories by means of counting methods", AGARDoGraph No. 292, paper 3.4, 1983.
- 3 D.J. Spiekhout, "Load monitoring of F-16A/B aircraft of the RNLAf with a smart electronic device", NLR TP 91116, 1991.
- 4 D.J. Spiekhout, "An Assessment of Fatigue Damage and Crack Growth Prediction Techniques", AGARD report R-797, Sept. 1993.
- 5 A.A. ten Have, "Usage monitoring of military helicopters", NLR TP 89276, AHS Oct. 1989.
- 6 M.L.W. Leenaarts, A.A. ten Have, "GEM cyclic life control: A smarter maintenance item within the Royal Netherlands Navy", NLR TP 96153, AHS June 1996.

- 7 J.B. de Jonge, "Acquisition of statistical gust load data by commercial airplanes", AGARD AG-317, May 1991.
- 8 J.B. de Jonge, *Reduction of Δn_z acceleration data to gust statistics*, NLR CR 92003 L, January 1992.
- 9 J.B. de Jonge, P.A. Hol, P.A. van Gelder, "Re-Analysis of European flight loads data", NLR TP 93535, November 1993.
- 10 P.A. van Gelder, "In-Flight Tail Load Measurements", (NLR TP 92158), ICAS-92-6.5.2
- 11 P.A. van Gelder, "Acquiring Tail Load Spectra from In-Flight Measurements", (NLR TP 93020), AIAA 93-1607

Symbols and abbreviations

\bar{x}	average value
σ_n	standard deviation
alt	(pressure) altitude (ft)
asym	anti-symmetrical part of stabilizer-root bending moment
bmom	stabilizer-root bending moment
elev	elevator deflection (deg)
epr	engine pressure ratio (average of left and right engine)
Eq.fl.	equivalent flight
symm	symmetrical part of stabilizer-root bending moment
FM	Flight Mode (see also table 1)
TE	Trailing Edge
T/R	Thrust Reverse